

Ultrafast Quantum Gates in Circuit QED

G. Romero,¹ D. Ballester,¹ Y. M. Wang,² V. Scarani,^{2,3} and E. Solano^{1,4}

¹*Departamento de Química Física, Universidad del País Vasco-Euskal Herriko Unibertsitatea, Apartado 644, 48080 Bilbao, Spain*

²*Centre for Quantum Technologies, National University of Singapore, 3 Science Drive 2, Singapore 117543*

³*Department of Physics, National University of Singapore, 2 Science Drive 3, Singapore 117542*

⁴*IKERBASQUE, Basque Foundation for Science, Alameda Urquijo 36, 48011 Bilbao, Spain*

(Dated: July 19, 2022)

We present a method of implementing ultrafast two-qubit gates valid for the ultrastrong coupling (USC) and deep strong coupling (DSC) regimes of light-matter interaction, considering state-of-the-art circuit quantum electrodynamics (QED) technology. Our proposal includes a suitable qubit architecture and is based on a four-step sequential displacement of an intracavity mode, operating at a time proportional to the inverse of the resonator frequency. Through *ab initio* calculations, we show that these quantum gates can be performed at subnanosecond time scales, while keeping the fidelity above 99%.

Introduction.—With the advent of quantum information science [1], there has been enormous efforts in the design of devices with high level quantum control and coherence [2]. Circuit QED [3–5] has become a leading technology for solid-state based quantum computation and its performance is approaching that of trapped ions [6] and all-optical implementations [7]. Considerable progress has been made in circuit QED experiments in recent years: ultrastrong coupling [8, 9], two-qubit gate and algorithms [11–16], three-qubit gate and entanglement [17, 18]. Most of the proposed gates are based on slow dispersive interactions or faster resonant gates, and would require operation times of about tens of nanoseconds.

To speed up gate operations, the latest circuit-QED technology offers the USC regime of light-matter interactions [8–10, 19, 20], where the coupling strength g is comparable to the resonator frequency ω_r ($0.1 \lesssim g/\omega_r \lesssim 1$). This should open the possibility to achieve ultrafast gates operating at subnanosecond time scales [21]. In this sense, the design of these novel gates becomes a challenge as the rotating-wave approximation (RWA) breaks down and the complexity of the quantum Rabi Hamiltonian emerges [22, 23]. Preliminary efforts have been done in this direction involving different configurations of superconducting circuits [24–26]. Likewise, in a recent contribution, it has been discussed the possibility of performing protected quantum computing [27].

In this letter, we propose a realistic scheme to realize ultrafast two-qubit controlled phase (CPHASE) gates between two newly designed flux qubits [28], coupled galvanically to a single-mode transmission line resonator (Fig. 1). Our proposal includes: (i) a CPHASE gate protocol operating at times proportional to the inverse of the resonator frequency; (ii) the design of the qubit-resonator system, allowing for high controllability on both the qubit transition frequency and the qubit-resonator coupling, in USC [8, 9] and potentially the DSC regime [29] of light-matter interaction. Through *ab initio* numerical analysis, we discuss the main features of this scheme in detail, and prove that the reached fidelity is within the required fault-tolerance for quantum computation [1].

Design of a versatile flux qubit.—The junction array is schematically depicted in Fig. 1. It consists of a six-Josephson-junctions configuration, each one denoted by a

cross, coupled galvanically [8, 9, 30] to a coplanar waveguide resonator — characterized by a superconducting phase difference $\Delta\psi$ — that supports a single mode of the electromagnetic field. The upper loop stands for a three-junction flux qubit [28], while the additional loops will allow a tunable qubit-resonator coupling strength. We analyze this qubit design in steps. First, we describe the potential energy coming from the inductive terms, which is the dominant contribution. Second, we describe the transmission line resonator inserted with a Josephson junction in the central line and introduce the superconducting phase slip $\Delta\psi$ across the junction shared with the resonator. Third, we add the capacitive terms which appear in the junctions and obtain the full Hamiltonian of the system using a standard procedure. Finally, we identify two levels in the degrees of freedom of the junction architecture, which will define our qubit, and obtain the effective Hamiltonian to describe the ultrafast two-qubit gate.

The potential energy due to the inductive terms is obtained

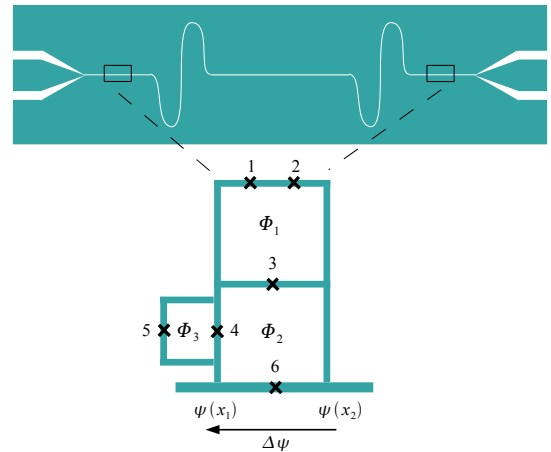


FIG. 1. (Color online) Circuit-QED configuration consisting on a six-Josephson-junctions array coupled galvanically to a single-mode resonator (bottom horizontal line). The flux qubit is defined by the three Josephson junctions in the upper loop threaded by an external flux Φ_1 . Two additional loops allow a tunable and switchable qubit-resonator coupling.

by adding the corresponding Josephson potentials $\mathcal{E}(\varphi_k) = -E_{Jk} \cos(\varphi_k)$, where E_{Jk} and φ_k represent the Josephson energy and the superconducting phase across the k -th junction, respectively. We assume $E_{J1} = E_{J2} \equiv E_J$, $E_{J3} = \alpha E_J$ and $E_{J4} = E_{J5} = \alpha_4 E_J$. In addition, around each closed loop the total flux has to be a multiple of the flux quantum $\Phi_0 = h/2e$, or expressed in terms of superconducting phases, $\sum_k \varphi_k = 2\pi f_j + 2\pi n$, where we defined the frustration parameter $f_j = \Phi_j/\Phi_0$ ($j = 1, 2, 3$). Using this quantization rule, the total potential energy U , containing both the qubit energy and the qubit-resonator interaction, reads

$$\frac{U}{E_J} = -[\cos \varphi_1 + \cos \varphi_2 + \alpha \cos(\varphi_2 - \varphi_1 + 2\pi f_1) + 2\alpha_4(f_3) \cos(\varphi_2 - \varphi_1 + 2\pi \tilde{f} + \Delta\psi)], \quad (1)$$

where $\alpha_4(f_3) \equiv \alpha_4 \cos(\pi f_3)$, $\tilde{f} = f_1 + f_2 + f_3/2$, and $\Delta\psi$ stands for the phase slip shared by the resonator and f_2 -loop. It is also noteworthy to mention that the junction at the central line introduces a boundary condition that modifies the mode structure of the resonator, but it does not alter the inductive potential (1). The parameters α , α_4 and f_j can be optimized for a suitable working point.

We introduce now the Hamiltonian of the interrupted inhomogeneous transmission line resonator. After the mapping the nonuniform resonator into a sum of harmonic oscillators, the standard Hamiltonian described by flux amplitude ψ_n and charge q_n as its conjugate momentum is [20]

$$\mathcal{H}_r = \sum_n \left(\frac{q_n^2}{2\tilde{C}_r} + \frac{\tilde{C}_r}{2} \omega_n^2 \psi_n^2 \right), \quad (2)$$

where $\tilde{C}_r = C_r + C_{J6}$ is the modified resonator capacitance due to the presence of the sixth Josephson junction at the central line, see Fig. 1. The quantization procedure yields

$$\mathcal{H}_r = \sum_n \hbar \omega_n (a_n^\dagger a_n + 1/2), \quad (3)$$

with $\omega_n = k_n/\sqrt{L_0 C_0}$ (C_0 , L_0 the capacitance and inductance per unit length, respectively), and $k_n = (2L_0/L_J)(1 - \omega_n^2/\omega_p^2) \cot(k_n l)$, where $\omega_p = 1/\sqrt{L_J C_J}$ is the plasma frequency of the junction and $2l$ is the length of the central line.

In the following, we restrict to the case that the junctions only interact with the first eigenmode of the resonator. The modified superconducting phase slip $\Delta\psi$ is related to the single-mode resonator variables as

$$\Delta\psi = \Delta\psi_1 (a + a^\dagger), \quad (4)$$

where $\Delta\psi_1 = (\delta_1/\varphi_0)(\hbar/2\omega_r \tilde{C}_r)^{1/2}$. Here, $\varphi_0 = \Phi_0/2\pi$ is the reduced flux quantum, ω_r is the frequency of the first eigenmode, $\delta_1 = u_1(x_2) - u_1(x_1)$ corresponds to the difference between the first-order spatial eigenmode, evaluated at points shared by the resonator and the f_2 -loop.

The total Hamiltonian is obtained by including the kinetic terms of the qubit and the Hamiltonian of the resonator

$$\mathcal{H} = 4AE_c(n_1^2 + n_2^2) + 8BE_c n_1 n_2 + \mathcal{H}_r + 2e \frac{C}{C_r} q_n (n_1 - n_2) + U(\varphi_1, \varphi_2), \quad (5)$$

where $E_c = e^2/2C_J$ is the charging energy, A, B, C are functions of system parameters [31] such as junctions size and phase slip magnitude. The degrees of freedom of the junction architecture are (φ_1, φ_2) and their conjugate momenta, which are the numbers (n_1, n_2) of Cooper pairs in the boxes.

In order to define a qubit within the junction architecture, we diagonalize the junctions-only part of the Hamiltonian. The two lowest energy eigenstates are labeled as the eigenstates of σ_z , and the two-dimensional subspace spanned by them describes the qubit. Furthermore, since $\Delta\psi_1 \ll 1$ is true in general, we expand the potential (1) up to the second order in $\Delta\psi$. This gives rise to the first-order and second-order qubit-resonator inductively coupling. Finally, after projecting the interaction terms also into the qubit basis, the Hamiltonian reads

$$\mathcal{H} = \frac{\hbar\omega_q}{2} \sigma_z + \hbar\omega_r a^\dagger a + \mathcal{H}_{\text{int}} \quad (6)$$

with the effective interaction Hamiltonian

$$\mathcal{H}_{\text{int}} = 2E_J \alpha_4(f_3) \sum_{m=1,2} (\Delta\psi)^m \sum_{\mu=x,y,z} c_\mu^m(\alpha, \alpha_4, f_1, f_2) \sigma_\mu, \quad (7)$$

the $c_\mu^m(\alpha, \alpha_4, f_1, f_2)$ are the controllable magnitudes of the longitudinal and transverse coupling strengths for m -th order interaction. Note that we ignore the capacitive coupling due to the fact that it is orders of magnitude smaller than the inductively coupling.

Numerical analysis.— We provide ab initio numerical examples to show the functionality of our setup. Firstly, we study the properties of the inhomogeneous transmission line resonator inserted by the sixth Josephson junction on the central line. The eigenfrequencies ω_n and eigenmodes $u_n(x)$ can be found numerically and calculated independently of the qubit Hamiltonian [20]. In fact, considering a resonator of impedance $Z \sim 50 \Omega$, capacitance $C_r \sim 850$ fF, and a Josephson capacitance $C_{J6} \sim 10$ fF, we estimate the first mode of the resonator with frequency $\omega_r/2\pi \sim 7$ GHz, which leads to a phase slip magnitude $\Delta\psi_1 = 0.1218$. These values determine the qubit-resonator coupling strength. Secondly, we perform the numerical study of the total Hamiltonian (5). It shows that, when external fluxes satisfies $f_2 + f_3/2 = 0.5$, both c_y^1 and the second-order coupling are negligible. This reduces the interaction Hamiltonian to

$$\mathcal{H}_{\text{int}} = \hbar g (a + a^\dagger) (c_z \sigma_z + c_x \sigma_x), \quad (8)$$

with the effective coupling strength $g = 2E_J \alpha_4(f_3) \Delta\psi_1/\hbar$ and $c_{z,x} \equiv c_{x,z}^1$.

Figure 2(a,b) shows c_z and c_x as a function of the qubit junction size α , and the frustration parameter f_1 . These two figures show clearly another characteristic of the setup, that is, the switching from transversal to longitudinal couplings depending on the external flux Φ_1 [10]. In particular, when selecting a qubit junction size $\alpha = 1.2$ and $f_1 = 0.505$, we have a large (small) contribution of longitudinal (transversal)

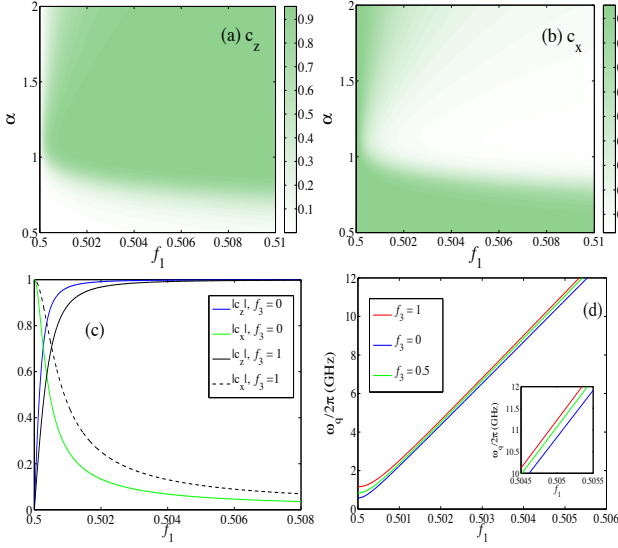


FIG. 2. (Color online) (a,b) Couplings strength c_z and c_x as a function of the qubit junction size $\alpha = E_{J3}/E_{J1}$, and the external frustration parameter $f_1 = \Phi_1/\Phi_0$, where Φ_0 is the flux quantum, for a frustration $f_3 = 0$. (c) Couplings strength for a qubit junction size $\alpha = 1.2$, and for values $f_3 = 0$ and $f_3 = 1$. (d) Qubit spectrum for values $f_3 = \{1, 0, 0.5\}$. In this simulation we have considered $E_J/h = 221$ GHz, a junction size $\alpha_4 = 0.058$.

coupling — see Fig. 2(c) where we plot c_z and c_x for a parameter $f_3 = 0$ and $f_3 = 1$.

From the diagonalization of qubit Hamiltonian for different values of the frustration parameter $f_3 = \{0, 1, 0.5\}$, we estimate a qubit frequency $\omega_q/2\pi \sim \{10.94, 11.25, 10.99\}$ GHz [see Fig. 2(d)]. Furthermore, considering a junction size $\alpha_4 = 0.058$ we estimate a qubit-resonator coupling strength as $g/\omega_r = \{0.446, -0.446, 0\}$, reaching the USC regime. It is noteworthy to mention that our setup allows us turning on and off the coupling g as well as to change the sign of it, operations that may be carried out in times about 0.1 ns [32].

The ratio g/ω_r could change at will without affecting the qubit properties required for the proposed protocol. For instance, for a junction size $\alpha_4 = 0.12$, a phase slip magnitude $\Delta\psi_n = 0.0835$ and a resonator frequency $\omega_r/2\pi \sim 8.7$ GHz (obtained from a central Josephson capacitance $C_{J6} \sim 19$ fF), one obtains $g/\omega_r = 0.509$. Also, with other choices of parameters, we could move from the USC to DSC regime and even the ratio of transversal to longitudinal coupling could be tuned. These examples, and particularly the model introduced by Eq. (8), will be the basis to develop protocols for ultrafast two-qubit gates.

Ultrafast two-qubit gate.— The external tunability of the previous circuit is now exploited to propose an ultrafast protocol for a two-qubit gate [21]. An interesting example of such a gate was introduced in Ref. [24]: a two-qubit CPHASE gate is produced by alternating between positive and negative values of the coupling strength g for each qubit. In our architecture, this can be done simply by changing the flux f_3 from 0 to 1; however, this action will also increase the

value of the undesired transversal coupling in Hamiltonian of Eq. (6). For instance, in case of a junction size $\alpha_4 = 0.058$, we find $g/\omega_r = \{0.446, -0.446\}$ and $c_x = \{0.055, 0.106\}$ for $f_3 = \{0, 1\}$.

The suitable protocol for the proposed realistic architecture, yielding to a fidelity within the required fault-tolerant quantum computing, consist of:

- Step 1.- The coupling g_1 is maximized ($f_3^{(1)} = 0$), whereas g_2 made exactly zero by tuning $f_3^{(2)} = 0.5$. The system evolves for a period $\omega_r t_1 \in (0, \pi/2]$.
- Step 2.- The coupling g_2 is maximized ($f_3^{(2)} = 0$), whereas g_1 made exactly zero by tuning $f_3^{(1)} = 0.5$. The system evolves for a period $\omega_r t_2 = \pi - \omega_r t_1$.
- Step 3.- Repeat Step 1.
- Step 4.- Repeat Step 2.

We study first the ideal case, in which the transversal component of the coupling in Eq. (6) is negligible, which could be achieved by tuning the fluxes $f_1 = 0.505$ of each qubit. Then, the two-qubit Hamiltonian is

$$\mathcal{H} = \sum_i \frac{\hbar\omega_{qi}}{2} \sigma_z^{(i)} + \hbar\omega_r a^\dagger a - \sum_i \hbar g_i (a + a^\dagger) \sigma_z^{(i)}. \quad (9)$$

Under this Hamiltonian, the unitary evolution operator \mathcal{U}_i corresponding to each step is

$$\begin{aligned} \mathcal{U}_{1,3} &= e^{-i \frac{\omega_{q1\uparrow} \sigma_z^{(1)} + \omega_{q2\downarrow} \sigma_z^{(2)}}{2} t_1} e^{-i\omega_r t_1 a^\dagger a} \mathcal{D} \left(\frac{g_1}{\omega_r} (e^{i\omega_r t_1} - 1) \sigma_z^{(1)} \right) \\ \mathcal{U}_{2,4} &= e^{-i \frac{\omega_{q1\downarrow} \sigma_z^{(1)} + \omega_{q2\uparrow} \sigma_z^{(2)}}{2} t_2} e^{-i\omega_r t_2 a^\dagger a} \mathcal{D} \left(\frac{g_2}{\omega_r} (e^{i\omega_r t_2} - 1) \sigma_z^{(2)} \right), \end{aligned} \quad (10)$$

where $\mathcal{D}(\beta\sigma_z) = \exp(\{\beta a^\dagger - \beta^* a\}\sigma_z)$ is a controlled coherent displacement of the field and $\omega_{qi\uparrow}, \omega_{qi\downarrow}$ stands for the value of the qubit frequency when g_i is maximum, zero, respectively. Finally, using $\mathcal{D}(\alpha)\mathcal{D}(\beta) = e^{i\text{Im}(\alpha\beta^*)}\mathcal{D}(\alpha + \beta)$ and $e^{-i\theta a^\dagger a}\mathcal{D}(\alpha)e^{i\theta a^\dagger a} = \mathcal{D}(\alpha e^{-i\theta})$, the gate $\mathcal{U} = \prod_i \mathcal{U}_i$ is

$$\begin{aligned} \mathcal{U} &= e^{-i(\omega_{q1\uparrow} t_1 + \omega_{q1\downarrow} t_2) \sigma_z^{(1)}} \\ &\times e^{-i(\omega_{q2\downarrow} t_1 + \omega_{q2\uparrow} t_2) \sigma_z^{(2)}} e^{4i \sin \omega_r t_1 \frac{g_1 g_2}{\omega_r^2} \sigma_z^{(1)} \sigma_z^{(2)}}. \end{aligned} \quad (11)$$

This gate \mathcal{U} is equivalent to a CPHASE quantum gate [1], up to local unitary operations, provided $4 \sin \omega_r t_1 g_1 g_2 / \omega_r^2 = \pi/4$ (notice that this condition requires g_i/ω_r to be in the ultrastrong regime). In the case of having a junction size $\alpha_4 = 0.058$, for which the coupling strength takes a value of $g_1/\omega_r = g_2/\omega_r = 0.446$ and $\omega_r \sim 2\pi \times 7.0$ GHz, then $\omega_r t_1 = 1.430$ and the total gating time will be $t_{\text{gate}} = 2\pi/\omega_r = 0.14$ ns.

Deviations from perfect fidelity are expected if one accounts for undesired transverse coupling in Eq. (6). For an initial state where both qubits are in the superposition

$|+\rangle = (|g\rangle + |e\rangle)/\sqrt{2}$ and the resonator in the vacuum, we can compute the fidelity of the state generated assuming that $c_x^{(i)} = 0.055$ for each qubit at $f_3^{(i)} = 0$. The fidelity of this state, as compared to the ideal state where this transverse coupling is neglected, amounts to $\mathcal{F} = 0.995$. For the sake of simplicity, we have considered instantaneous changes in the value of the fluxes f_3 . In this sense, the scheme can be easily adapted to account for smooth time-dependent profiles in the value of the coupling strength of both qubits. Indeed, driving frequencies of about 10 – 80 GHz are already available [32]. This should allow the experimental realization of a high-fidelity ultrafast CPHASE gate with subnanosecond operation time.

Discussion.—Given the CPHASE gate we proposed, based on the tunable qubit-resonator coupling in USC, we may consider the following extensions. (i) Multi-qubit entanglement and gate operations, such as realization of three-qubit Toffoli gates in the USC regime, faster than other schemes working in the strong coupling regime [18, 33]. (ii) With the advantage of switchable coupling in both strength and orientation, we may think of the generation of Ising-type Hamiltonian for qubit arrays. (iii) By controlling the geometric-related flux values, we can increase the higher-order couplings and thus study the nonlinear dynamics in USC regime. (iv) The adjustable coupling also allows us to couple to slower measurement devices.

Conclusion.—We have proposed a realistic scheme for implementing an ultrafast two-qubit CPHASE gate that may work with current circuit-QED technology. This gate may work at subnanosecond scale with fidelity $\mathcal{F} = 0.995$, which is within the requirements for fault-tolerant quantum computing. This proposal may lead to a significant improvement in the operating time when compared to standard circuit-QED scenarios, as well as microwave/optical cavity QED systems.

We thank P. Forn-Díaz, B. Peropadre, J. J. García-Ripoll, M. S. Kim, and C. M. Wilson, for useful discussions. This work was supported by the National Research Foundation and the Ministry of Education, Singapore, Juan de la Cierva MICINN Program, Spanish MICINN FIS2009-12773-C02-01, Basque Government IT472-10, SOLID, and CCQED European projects.

-
- [1] M. A. Nielsen and I. L. Chuang, *Quantum Computation and Quantum Information* (Cambridge University Press, Cambridge, 2000).
 [2] T. D. Ladd, F. Jelezko, R. Laflamme, Y. Nakamura, C. Monroe, and J. L. O’Brien, *Nature* **464**, 45 (2010).
 [3] A. Blais *et al.*, *Phys. Rev. A* **69**, 062320 (2004).
 [4] A. Wallraff *et al.*, *Nature (London)* **431**, 162 (2004).
 [5] I. Chiorescu *et al.*, *Nature (London)* **431**, 159 (2004).
 [6] D. Leibfried, R. Blatt, C. Monroe, and D. Wineland, *Rev. Mod. Phys.* **75**, 281 (2003).

- [7] P. Kok, W. J. Munro, K. Nemoto, T. C. Ralph, J. P. Dowling, and G. J. Milburn, *Rev. Mod. Phys.* **79**, 135 (2007).
 [8] T. Niemczyk, F. Deppe, H. Huebl, E. P. Menzel, F. Hocke, M. J. Schwarz, J. J. García-Ripoll, D. Zueco, T. Hümmer, E. Solano, A. Marx, and R. Gross, *Nature Phys.* **6**, 772 (2010).
 [9] P. Forn-Díaz, J. Lisenfeld, D. Marcos, J. J. García-Ripoll, E. Solano, C. J. P. M. Harmans, and J. E. Mooij, *Phys. Rev. Lett.* **105**, 237001 (2010).
 [10] B. Peropadre, P. Forn-Díaz, E. Solano, and J. J. García-Ripoll, *Phys. Rev. Lett.* **105**, 023601 (2010).
 [11] J. H. Plantenberg *et al.*, *Nature* **447**, 836 (2007).
 [12] L. DiCarlo *et al.*, *Nature* **460**, 240 (2009).
 [13] T. Yamamoto *et al.*, *Phys. Rev. B* **82**, 184515 (2010).
 [14] R. C. Bialczak *et al.*, *Nature Phys.* **6**, 409 (2010).
 [15] M. R. Geller, E. J. Pritchett, A. Galiutdinov, and J. M. Martinis, *Phys. Rev. A* **81**, 012320 (2010).
 [16] G. Haack, F. Helmer, M. Mariani, F. Marquardt, and E. Solano, *Phys. Rev. B* **82**, 024514 (2010).
 [17] L. DiCarlo *et al.*, *Nature* **467**, 574 (2010); M. Neeley *et al.*, *Nature* **467**, 570 (2010);
 [18] V. M. Stojanovic, A. Fedorov, C. Bruder, and A. Wallraff, arXiv:1108.3442.
 [19] C. Ciuti, G. Bastard, and I. Carusotto, *Phys. Rev. B* **72**, 115303 (2005).
 [20] J. Bourassa, J. M. Gambetta, A. A. Abdumalikov, Jr., O. Astafiev, Y. Nakamura, and A. Blais, *Phys. Rev. A* **80**, 032109 (2009).
 [21] See, as a reference, the proposed ultrafast gates in trapped ions: J. J. García-Ripoll, P. Zoller, and J. I. Cirac, *Phys. Rev. Lett.* **91**, 157901 (2003); J. J. García-Ripoll, P. Zoller, and J. I. Cirac, *Phys. Rev. A* **71**, 062309 (2005).
 [22] D. Braak, *Phys. Rev. Lett.* **107**, 100401 (2011).
 [23] E. Solano, *Physics* **4**, 68 (2011).
 [24] Y. D. Wang, P. Zhang, D. L. Zhou, and C. P. Sun, *Phys. Rev. B* **70**, 224515 (2004).
 [25] Y. D. Wang, A. Kemp, and K. Semba, *Phys. Rev. B* **79**, 024502 (2009).
 [26] Y. D. Wang, S. Chesi, D. Loss, and C. Bruder, *Phys. Rev. B* **81**, 104524 (2010).
 [27] P. Nataf and C. Ciuti, arXiv:1106.1159.
 [28] T. P. Orlando, J. E. Mooij, L. Tian, C. H. Van der Wal, L. S. Levitov, S. Lloyd, and J. J. Mazo, *Phys. Rev. B* **60**, 15398 (1999).
 [29] J. Casanova, G. Romero, I. Lizuain, J. J. García-Ripoll, and E. Solano, *Phys. Rev. Lett.* **105**, 263603 (2010).
 [30] A. A. Abdumalikov, O. Astafiev, Y. Nakamura, Y. A. Pashkin, and J. S. Tsai, *Phys. Rev. B* **78**, 180502 (2008).
 [31] The values of A, B, and C, read

$$A = \frac{\tilde{C}_r(1 + \alpha + 2\alpha_4) + 2\alpha_4 \delta_1^2 C_J(1 + \alpha)}{\tilde{C}_r(1 + (\alpha + 2\alpha_4)) + 2\alpha_4 \delta_1^2 C_J(1 + 2\alpha)}$$

$$B = \frac{2\alpha\alpha_4 C_J \delta_1^2 + \tilde{C}_r(\alpha + 2\alpha_4)}{\tilde{C}_r(1 + 2(\alpha + 2\alpha_4)) + 2\alpha_4 \delta_1^2 C_J(1 + 2\alpha)}$$

$$C = \frac{2\tilde{C}_r \alpha_4 \delta_1}{\tilde{C}_r(1 + 2(\alpha + 2\alpha_4)) + 2\alpha_4 \delta_1^2 C_J(1 + 2\alpha)}$$

- [32] C. M. Wilson, G. Johansson, A. Pourkabirian, J. R. Johansson, T. Duty, F. Nori, P. Delsing, arXiv:1105.4714v1; C. M. Wilson. Private communication.
 [33] A. Fedorov, L. Steffen, M. Baur, and A. Wallraff arXiv:1108.3966.